Electromagnetic excitations of a small gyrotropic sphere

G. W. Ford
Physics Department, University of Michigan, Ann Arbor, Michigan 48104

J. K. Furdyna*
Physics Department, Purdue University, West Lafayette, Indiana 47907

S. A. Werner
Physics Department, Scientific Research Staff, Ford Motor Company, Dearborn, Michigan 48121, and Department of Nuclear Engineering, University of Michigan, Ann Arbor, Michigan 48105

(Received 28 January 1975)

Theoretical expressions for the microwave power absorbed in a small spherical magnetoplasma are obtained using a perturbation expansion in powers of a dimensionless parameter proportional to the square of the radius. There are four linearly independent orientations of the microwave electric and magnetic fields ($\vec{E}_1$ and $\vec{B}_1$) relative to the dc magnetic field $\vec{B}_0$: transverse magnetic ($\vec{B}_1 \perp \vec{B}_0$), longitudinal magnetic ($\vec{B}_1 \| \vec{B}_0$), transverse electric ($\vec{E}_1 \perp \vec{B}_0$), and longitudinal electric ($\vec{E}_1 \| \vec{B}_0$). The theory includes the effects of electron inertia, displacement current, and the averages over the energy-dependent electron relaxation time. If the relaxation time is energy independent, in the limit of very small radius (Rayleigh limit), the result for the transverse electric case becomes the well-known formula for plasma-shifted cyclotron resonance. The results are applied to explain the microwave experiments on small spheres of n-type InSb by Evans, Furdyna, and Galeener. The calculation accounts quantitatively for (a) the position and shape of the plasma-shifted cyclotron resonance, (b) the fact that the longitudinal electric absorption is negligible, (c) the position, shape, and size dependence of the transverse magnetic resonance, and (d) the broad absorption shoulder observed in the longitudinal magnetic case. It is proposed that with this theory it is now possible to measure accurately in a single microwave experiment all four macroscopic electrical parameters of a given sample: mobility, carrier effective mass, lattice dielectric constant, and carrier density.

I. INTRODUCTION

Recently, Evans, Furdyna and Galeener[1,2] have observed a new type of microwave resonant absorption in small spheres of n-type InSb. The experiment involves placing the sphere in a dc magnetic field $\vec{B}_0$ and exciting it with microwaves. The microwave power absorbed in the sphere depends on the relative orientation of $\vec{B}_0$ and the microwave electric and magnetic fields $\vec{E}_1$ and $\vec{B}_1$, respectively. There are four linearly independent excitations: transverse magnetic ($\vec{B}_1 \perp \vec{B}_0$), longitudinal magnetic ($\vec{B}_1 \| \vec{B}_0$), transverse electric ($\vec{E}_1 \perp \vec{B}_0$), and longitudinal electric ($\vec{E}_1 \| \vec{B}_0$). These excitations can be observed separately, or simultaneously in various combinations, by appropriate choice of magnet orientation and location of the sample in the microwave cavity.

The experimental results are illustrated by Fig. 1, which shows microwave power absorbed as a function of B_0 for two geometries: transverse electric plus longitudinal magnetic and transverse magnetic plus longitudinal electric. The well-known plasma-shifted cyclotron resonance is observed in the case of transverse electric excitation,[3] but with a width about twice that expected from the dc mobility. In addition, in the same experimental curve there is an unexplained broad absorption shoulder near zero B_0 associated with longitudinal magnetic excitation. The new resonance is that observed in the transverse-magnetic plus longitudinal-electric geometry. For very small spheres this resonance occurs at a value of the cyclotron frequency ω_c ($= eB_0/m^*c$) which is independent of sphere radius, carrier concentration, and mobility. Although the quantitative behavior of this resonance was not understood, it was clear that, once understood, it would provide a new means for measuring m^*, the effective mass. It was also demonstrated that, with increasing radius, this resonance gradually transforms into a size-dependent helicon resonance.

Our purpose in this paper is to present a unified electromagnetic calculation which explains all of these results. For the experiments of interest here, the radius of the sphere a is always very small compared to the free-space wavelength λ of the microwave field,

$$a/\lambda \ll 1. \tag{1}$$

In this limit an exact calculation is possible.[4]

In the present case, the smallest spheres (those displaying the behavior of Fig. 1) also satisfy the Rayleigh limit,[5] where the microwave-field distribution in the *interior* of the sphere is nearly uniform. A rough criterion for the validity of the Rayleigh limit is that the sphere radius be small

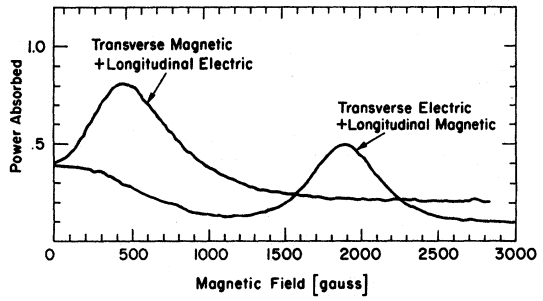

FIG. 1. Microwave absorption in a small sphere of n-type InSb as a function of magnetic field as measured for the two configurations: ($\vec{B}_1 \perp \vec{B}_0$, $\vec{E}_1 \parallel \vec{B}_0$) and ($\vec{E}_1 \perp \vec{B}_0$, $\vec{B}_1 \parallel \vec{B}_0$). The experiment was done at 78 K at a frequency of 35.2 GHz. The carrier concentration is about $5.2\times 10^{13}/\mathrm{cm}^3$, the sphere radius is 0.00838 cm, and the mobility is approximately 11×10^5 cm^2/V sec.

compared to the classical skin depth $\delta = c/(2\pi\omega\sigma_0)^{1/2}$, where σ_0 is the dc conductivity at $B_0 = 0$.

We will obtain a solution in the form of an expansion about this limit in ascending powers of a, and will calculate the first two terms in this expansion. The result yields closed-form expressions for the power absorbed from the microwave fields. It will be seen that this result holds reasonably well even for spheres whose radius considerably exceeds the above Rayleigh-limit criterion. It is hoped that these calculations will be more illuminating than the exact solution, which cannot be given in closed form.

In Sec. II we write down the basic equations for this problem; the effects of electron inertia, an energy-dependent relaxation time, and displacement current are included. Then in Sec. III we solve these equations for the case of magnetic excitation, using a perturbation scheme to obtain a solution in powers of a. The electric-excitation problem is solved by the same technique in Sec. IV. In Sec. V these results are discussed in various limits. Section VI is devoted to an application of these results to the experiments of Evans, Furdyna, and Galeener.

The microwave absorption depends upon four macroscopic electrical parameters: the dc mobility μ, the lattice dielectric constant ϵ_l, the carrier concentration N, and the carrier effective mass m^*; and in addition, on the energy dependence of the carrier relaxation time $\tau(\mathcal{E})$. Assuming this energy dependence to be that characteristic of Rutherford scattering of electrons by ionized impurities, we find that both the transverse-electric and transverse-magnetic resonance structures can be fit with one set of the four parameters. Thus, a unique advantage of this type of experiment is that all four electrical parameters can be determined from a single experiment on a given sample. It is, of course, especially important that these parameters include m^* and ϵ_l.

II. BASIC EQUATIONS

In this section we combine Maxwell's equations and a generalized form of the Ohm-Hall law in order to establish the basic equations and the appropriate boundary conditions for a gyrotropic sphere.

A. Generalized Ohm-Hall law

For fields varying as $e^{-i\omega t}$, the *total* current density is

$$\vec{J} = \vec{j} - i(\omega\epsilon_l/4\pi)\vec{E} , \tag{2}$$

where $\vec{j}$ is the conduction current density and the second term is the displacement current density. The connection between the conduction current density $\vec{j}$ and the electric field $\vec{E}$ is obtained from the Boltzmann equation using standard methods; the result can be written[6]

$$\vec{j} = [C_1 + i(\omega\epsilon_l/4\pi)]\vec{E} + C_2\,\hat{z}\cdot\vec{E}\hat{z} + C_3\,\hat{z}\times\vec{E} , \tag{3}$$

where the dc field $\vec{B}_0$ has been taken to be directed along the positive z axis. For a single isotropic parabolic band the coefficients C_j are given by

$$C_1 = \frac{Ne^2}{m^*}\left\langle \frac{\tilde{\tau}}{1+(\omega_c\tilde{\tau})^2}\right\rangle - i\frac{\omega\epsilon_l}{4\pi} , \tag{4a}$$

$$C_2 = \frac{Ne^2}{m^*}\left\langle \frac{\omega_c^2\tilde{\tau}^3}{1+(\omega_c\tilde{\tau})^2}\right\rangle , \tag{4b}$$

$$C_3 = \frac{Ne^2}{m^*}\left\langle \frac{\omega_c\tilde{\tau}^2}{1+(\omega_c\tilde{\tau})^2}\right\rangle , \tag{4c}$$

where $\langle\ \rangle$ means the following average over energy $\mathcal{E}$:

$$\langle F\rangle = \int_0^\infty d\mathcal{E}\, F\mathcal{E}^{3/2}\frac{\partial f_0}{\partial\mathcal{E}} \Big/ \int_0^\infty d\mathcal{E}\,\mathcal{E}^{3/2}\frac{\partial f_0}{\partial\mathcal{E}} . \tag{5}$$

Here f_0 is the Fermi-Dirac distribution function, and $\tilde{\tau}$ is related to the energy-dependent relaxation time $\tau(\mathcal{E})$ by

$$\tilde{\tau}(\mathcal{E}) = \tau(\mathcal{E})/[1 - i\omega\tau(\mathcal{E})] . \tag{6}$$

Putting (3) into (2) and solving for $\vec{E}$ in terms of $\vec{J}$, we can write

$$\tilde{\sigma}\vec{E} = \vec{J} + \tilde{\gamma}\hat{z}\cdot\vec{J}\hat{z} + \tilde{W}\hat{z}\times\vec{J} , \tag{7}$$

where

$$\begin{aligned} \tilde{\sigma} &= (C_1^2 + C_3^2)/C_1 , \\ \tilde{\gamma} &= (C_3^2 - C_1C_2)/C_1(C_1 + C_2) , \\ \tilde{W} &= -C_3/C_1 . \end{aligned} \tag{8}$$

We call (7) the generalized Ohm-Hall law. This is the basic constitutive relation connecting $\vec{E}$ with $\vec{J}$.

B. Maxwell's equations

Inside the sphere, the equations which we must solve are Ampere's circuital law (for a medium

of unit permeability)

$$\text{curl}\vec{B} = (4\pi/c)\vec{J}\,, \tag{9}$$

and Faraday's magnetic induction law

$$\text{curl}\vec{E} = i(\omega/c)\vec{B}\,. \tag{10}$$

Substituting the expression for $\vec{E}$ from (7) into (10) we have

$$\text{curl}(\vec{J} + \tilde{\gamma}\hat{z}\cdot\vec{J}\hat{z} + \tilde{W}\hat{z}\times\vec{J}) = i(\omega\tilde{\sigma}/c)\vec{B}\,. \tag{11}$$

Eliminating $\vec{B}$ between this expression and (9), we get

$$\text{curl}\,\text{curl}(\vec{J} + \tilde{\gamma}\hat{z}\cdot\vec{J}\hat{z} + \tilde{W}\hat{z}\times\vec{J}) - \tilde{q}_0^2\vec{J} = 0\,, \tag{12}$$

where the complex wave vector is defined by

$$\tilde{q}_0^2 \equiv i(4\pi\omega\tilde{\sigma}/c^2)\,. \tag{13}$$

Equation (12) is a generalization of the helicon wave equation discussed in an earlier paper by two of us.[7] The essential differences arise from the inclusion of the effects of electron inertia, displacement current, and the energy dependence of the relaxation time. These result in the additional term $\tilde{\gamma}\hat{z}\cdot\vec{J}\hat{z}$, and the fact that $\tilde{W}$ and $\tilde{\sigma}$ are now complex, hence the tilde on these quantities.

The key simplification arising from our assumption (1) is in the equations for the fields *outside the sphere*. For the case when the exciting field is an ac magnetic field, we neglect the displacement current [right-hand side of (9)]. The magnetic field then satisfies the quasistatic equations:

$$\text{curl}\vec{B} = 0 \quad\text{and}\quad \text{div}\vec{B} = 0\,; \tag{14}$$

the electric field is ignored. On the other hand, when the exciting field is an ac electric field, we neglect the magnetic-induction field [right-hand side of (10)]. The electric field then satisfies the quasistatic equations

$$\text{curl}\vec{E} = 0 \quad\text{and}\quad \text{div}\vec{E} = 0\,; \tag{15}$$

the magnetic field is ignored.

Because in the case of magnetic excitation we solve for $\vec{B}$ and ignore $\vec{E}$, and vice versa in the case of electric excitation, the boundary conditions to be applied are different in the two cases. At the surface of the sphere ($r = a$), we must have

$$\vec{B}_{\text{inside}} = \vec{B}_{\text{outside}}\ \text{(magnetic excitation)}, \tag{16}$$

and

$$(\vec{J}\cdot\hat{r})_{\text{inside}} = (\vec{J}\cdot\hat{r})_{\text{outside}}, \tag{17a}$$

$$(\hat{r}\times\vec{E})_{\text{inside}} = (\hat{r}\times\vec{E})_{\text{outside}} \Big\}\ \text{(electric excitation)}. \tag{17b}$$

These boundary conditions are obtained directly from (9) and (10) using standard arguments.

III. MAGNETIC EXCITATION

Here we obtain, in the form of a perturbation expansion, the response of a gyrotropic sphere to a uniform ac magnetic field $\vec{B}_1 e^{-i\omega t}$. The essential difficulty of this problem is the nonseparability of the basic equations of Sec. II in spherical coordinates. Although this means that the calculation is fairly complicated, the final results for the power absorbed have a rather simple explicit form.

A. Perturbation scheme

We seek a series solution for $\vec{B}(\vec{r})$ and $\vec{J}(\vec{r})$ in the form

$$\vec{B} = \vec{B}^{(0)} + \vec{B}^{(1)} + \vec{B}^{(2)} + \cdots\,, \tag{18}$$

and

$$\vec{J} = \vec{J}^{(0)} + \vec{J}^{(1)} + \vec{J}^{(2)} + \cdots\,. \tag{19}$$

The expansion is in powers of the dimensionless parameter $\tilde{V}$ defined by

$$\tilde{V} \equiv 4\pi\omega\tilde{\sigma}a^2/c^2\,, \tag{20}$$

that is,

$$\vec{B}^{(n)} \ \text{ and } \ \vec{J}^{(n)} \propto \tilde{V}^n\,. \tag{21}$$

We note that (9) and (10) require

$$\text{div}\vec{B}^{(n)} = 0 \ \text{ and } \ \text{div}\vec{J}^{(n)} = 0\,. \tag{22}$$

At very low frequency (or very small radius), the applied ac magnetic field penetrates the sphere uniformly (Rayleigh limit), so that in zeroth order

$$\vec{B}^{(0)} = \vec{B}_1\,, \tag{23}$$

both inside and outside the sphere. In zeroth order, the current density $\vec{J}^{(0)} = 0$. The first-order current density $\vec{J}^{(1)}$ is obtained by solving (11), where the source of these currents is $\vec{B}^{(0)}$ given by (23),

$$\text{curl}(\vec{J}^{(1)} + \tilde{\gamma}\hat{z}\cdot\vec{J}^{(1)}\hat{z} + \tilde{W}\hat{z}\times\vec{J}^{(1)}) = (i\omega\tilde{\sigma}/c)\vec{B}^{(0)}\,. \tag{24}$$

This first-order current then gives rise to a new magnetic field $\vec{B}^{(1)}$ which, inside the sphere, is found by solving (9):

$$\text{curl}\vec{B}^{(1)} = \frac{4\pi}{c}\vec{J}^{(1)}\,. \tag{25}$$

Outside the sphere $\vec{B}^{(1)}$ is found by solving (14) and satisfying the boundary condition (16).

This first-order magnetic field then gives rise to a second order current which is calculated by again solving (11), where the source term is now the known function $\vec{B}^{(1)}$,

$$\text{curl}(\vec{J}^{(2)} + \tilde{\gamma}\hat{z}\cdot\vec{J}^{(2)}\hat{z} + \tilde{W}\hat{z}\times\vec{J}^{(2)}) = i(\omega\tilde{\sigma}/c)\vec{B}^{(1)}\,. \tag{26}$$

The second order magnetic field inside the spheres is found by again solving (9), where the known function $\vec{J}^{(2)}$ is the source term appearing on the right-hand side, namely,

$$\mathrm{curl}\vec{B}^{(2)} = (4\pi/c)\vec{J}^{(2)} \ . \tag{27}$$

This field is continued to the region outside the sphere by finding a solution of (14) which satisfies the boundary condition (16).

The above scheme can, in principle, be carried to all orders, leading to expressions for $\vec{J}$ and $\vec{B}$ in the form of a power series in $\tilde{V}$.

B. First-order solution

Note first that, since the right-hand side of (24) is a constant, $\vec{J}^{(1)}$ is linear in $\vec{r}$. Moreover, the divergence of $\vec{J}^{(1)}$ is zero, which in turn requires $\hat{r}\cdot\vec{J}^{(1)} = 0$ at the surface of the sphere, since we take $\vec{J}^{(1)}$ to be zero outside the sphere. Therefore, we conclude that the solution of (24) must be of the form

$$\vec{J}^{(1)} = \vec{K}\times\vec{r} \quad (r<a) \ . \tag{28}$$

The constant vector $\vec{K}$ is determined by direct substitution of (28) into (24) and solving the resulting vector equation; we get

$$\vec{K} = i\frac{\omega\tilde{\sigma}}{c}\left(\tfrac{1}{2}\hat{z}\cdot\vec{B}_1\hat{z} + \frac{2+\tilde{\gamma}}{(2+\tilde{\gamma})^2+\tilde{W}^2}(\vec{B}_1 - \hat{z}\cdot\vec{B}_1\hat{z}) - \frac{\tilde{W}}{(2+\tilde{\gamma})^2+\tilde{W}^2}\hat{z}\times\vec{B}_1\right) . \tag{29}$$

The solution of the succeeding equations is considerably simplified by the introduction of the vector spherical harmonics $\vec{Y}^m_{L,l}$. These vector functions are defined in Appendix A. We also make extensive use of the formulas given in Appendix B of Ref. 7. We begin by expressing the result contained in (28) and (29) in terms of these vector functions:

$$\vec{J}^{(1)} = \left(\frac{8\pi}{3}\right)^{1/2}\frac{\tilde{\sigma}\omega}{c}\sum_{m=-1}^{+1}\frac{\hat{e}^*_m\cdot\vec{B}_1}{2+m^2\tilde{\gamma}-im\tilde{W}}\, r\vec{Y}^m_{1,1} \ , \tag{30}$$

where the complex unit vectors $\hat{e}_m$ are defined in Appendix A and the * means complex conjugation. This result is easily verified by noting

$$r\vec{Y}^m_{1,1} = i\left(\frac{3}{8\pi}\right)^{1/2|}\hat{e}_m\times\vec{r} \ , \tag{31}$$

which in turn is most directly obtained from Eq. (B8) of Ref. 7.

We now use the result (30) to solve (25) for $\vec{B}^{(1)}$ inside the sphere. Since $\vec{J}^{(1)}$ is linear in $\vec{r}$, $\vec{B}^{(1)}$ inside the sphere can only involve terms quadratic in $\vec{r}$ plus a constant. By examining the formulas for curl and divergence in Appendix B of Ref. 7, it is relatively easy to show that the first-order magnetic field which satisfies the boundary condition (16) is

$$\vec{B}^{(1)} = -i(2\pi)^{1/2}\frac{\tilde{V}}{15}\sum_{m=-1}^{+1}\frac{\hat{e}^*_m\cdot\vec{B}_1}{1+\frac{1}{2}m^2\tilde{\gamma}-\frac{1}{2}im\tilde{W}}\begin{cases}(5/\sqrt{2})[(r^2/a^2)-1]\vec{Y}^m_{1,0}+(r^2/a^2)\vec{Y}^m_{1,2}, & r<a\\ (a/r)^3\vec{Y}^m_{1,2}, & r>a\end{cases} \ . \tag{32}$$

The first-order magnetic induction field outside the sphere is therefore a pure dipole field (see Sec. III B of Ref. 7).

C. Second-order solution

The problem now becomes more complicated. We must solve (26) for $\vec{J}^{(2)}$, with the right-hand side of this equation given by (32). Since the magnetic field $\vec{B}^{(1)}$ is of even parity, involving terms independent of r and quadratic in r, $\vec{J}^{(2)}$ must be of odd parity, involving terms linear and cubic in r. The most general form for $\vec{J}^{(2)}$ having zero divergence is

$$\vec{J}^{(2)} = \sum_{m=-1}^{+1}\{(b^m_1a^2r + b^m_2r^3)\vec{Y}^m_{1,1} + b^m_3[\sqrt{\tfrac{2}{5}}r^3\vec{Y}^m_{2,3} + \tfrac{1}{2}\sqrt{\tfrac{3}{5}}r(7r^2-5a^2)\vec{Y}^m_{2,1}] + b^m_4r^3\vec{Y}^m_{3,3}] \ . \tag{33}$$

The particular combination of terms multiplying b^m_3 is obtained by noting that because $\vec{J}^{(2)}$ has zero divergence and $\vec{J}$ is zero outside the sphere in all orders, $\hat{r}\cdot\vec{J}^{(2)}$ is zero at the surface of the sphere. The four undetermined coefficients b^m_1, b^m_2, b^m_3, and b^m_4 are found by first using the formulas for $\hat{z}\times\vec{Y}^m_{L,l}$ in Appendix B of Ref. 7 and for $\hat{z}\cdot\vec{Y}^m_{L,l}\hat{z}$ in Appendix A to form the sum

$$\vec{J}^{(2)} + \tilde{\gamma}\hat{z}\cdot\vec{J}^{(2)}\hat{z} + \tilde{W}\hat{z}\times\vec{J}^{(2)} \ , \tag{34}$$

calculating the curl of this sum, and equating the result to $i(\omega\tilde{\sigma}/c)\vec{B}^{(1)}$ as required by (26). The expression for the curl of the sum (34) involves four vector spherical harmonics $\vec{Y}^m_{1,0}$, $\vec{Y}^m_{1,2}$, $\vec{Y}^m_{2,2}$, and $\vec{Y}^m_{3,2}$; the result (32) for $\vec{B}^{(1)}$ contains $\vec{Y}^m_{1,0}$ and $\vec{Y}^m_{1,2}$. Thus, in order to satisfy (26) we must separately equate the coefficients of these four vector spherical harmonics on each side of the equation. This gives the four equations necessary to find the coefficients b^m_j. In matrix form these equations are

$$\begin{bmatrix} \beta_1 & 0 & -\frac{5}{4}\beta_2 & 0 \\ 0 & \beta_1 & \frac{7}{4}\beta_2 & 0 \\ 0 & \beta_2 & \beta_3 & \frac{7}{3}\beta_4 \\ 0 & 0 & \frac{1}{3}\beta_4 & \beta_5 \end{bmatrix} \begin{bmatrix} b_1^m \\ b_2^m \\ b_3^m \\ b_4^m \end{bmatrix} = i\left(\frac{2\pi}{3}\right)^{1/2} \frac{\omega\tilde{\sigma}\tilde{V}\hat{e}_m^* \cdot \vec{B}_1}{30ca^2\beta_1} \begin{bmatrix} 5 \\ -3 \\ 0 \\ 0 \end{bmatrix}, \tag{35}$$

where

$$\beta_1 = 1 + \tfrac{1}{2}m^2\tilde{\gamma} - \tfrac{1}{2}im\tilde{W}, \tag{36a}$$

$$\beta_2 = [\tfrac{1}{5}(4-m^2)]^{1/2}(m\tilde{\gamma} + i\tilde{W}), \tag{36b}$$

$$\beta_3 = 7 + (4 - \tfrac{5}{6}m^2)\tilde{\gamma} - i\tfrac{7}{6}m\tilde{W}, \tag{36c}$$

$$\beta_4 = [(9-m^2)/70]^{1/2}(-m\tilde{\gamma} + 4i\tilde{W}), \tag{36d}$$

$$\beta_5 = 1 + \tfrac{1}{12}m^2\tilde{\gamma} - i\tfrac{1}{12}m\tilde{W}. \tag{36e}$$

The solution of (35) is

$$\begin{bmatrix} b_1^m \\ b_2^m \\ b_3^m \\ b_4^m \end{bmatrix} = i\left(\frac{2\pi}{3}\right)^{1/2} \frac{\omega\tilde{\sigma}\tilde{V}\hat{e}_m^* \cdot \vec{B}_1}{30ca^2\beta_1\xi} \begin{bmatrix} -3(\beta_3\beta_5 - \frac{7}{9}\beta_4^2) \\ 3\beta_2\beta_5 \\ -\beta_2\beta_4 \\ \beta_1\beta_3\beta_5 - \frac{7}{9}\beta_1\beta_4^2 - \beta_5\beta_2^2 \end{bmatrix}, \tag{37}$$

where

$$\xi = \beta_1\beta_3\beta_5 - \tfrac{7}{9}\beta_1\beta_4^2 - \tfrac{7}{4}\beta_5\beta_2^2. \tag{38}$$

To find the second-order magnetic field inside the sphere we must solve (27), where the source term $\vec{J}^{(2)}$ is now known. Following the technique used in obtaining the first-order solution, we find for $r < a$

$$\vec{B}^{(2)} = i\frac{4\pi}{c}\sum_{m=-1}^{+1}\{b_1^m a^2[\tfrac{1}{2}\sqrt{\tfrac{2}{3}}(r^2-a^2)\vec{Y}_{1,0}^m + \tfrac{1}{5}\sqrt{\tfrac{1}{3}}r^2\vec{Y}_{1,2}^m] + b_2^m[\tfrac{1}{4}\sqrt{\tfrac{2}{3}}(r^4-a^4)\vec{Y}_{1,0}^m + \tfrac{1}{7}\sqrt{\tfrac{1}{3}}r^4\vec{Y}_{1,2}^m]$$
$$+ b_3^m\tfrac{1}{2}r^2(r^2-a^2)\vec{Y}_{2,2}^m + b_4^m r^2[\tfrac{1}{2}\sqrt{\tfrac{4}{7}}(r^2-a^2)\vec{Y}_{3,2}^m + \tfrac{1}{9}\sqrt{\tfrac{3}{7}}r^2\vec{Y}_{3,4}^m]\}. \tag{39}$$

The solution for the second-order magnetic field outside the sphere, which satisfies (14) and the boundary condition (16), is

$$\vec{B}^{(2)} = -i\frac{4\pi}{c}a^4\sum_{m=-1}^{+1}\left[\sqrt{\tfrac{1}{3}}(\tfrac{1}{5}b_1^m + \tfrac{1}{7}b_2^m)\left(\frac{a}{r}\right)^3\vec{Y}_{1,2}^m + \tfrac{1}{9}\sqrt{\tfrac{3}{7}}b_4^m\left(\frac{a}{r}\right)^5\vec{Y}_{3,4}^m\right]. \tag{40}$$

The term involving $\vec{Y}_{3,4}^m$ is an octupole field. Thus, we see that this second-order calculation results in a correction to the dipole field [first term in (40)] and the appearance of an octupole contribution. The even-l 2^l-pole fields are zero in all orders, as can be established from inversion symmetry. We will not carry the calculation beyond this point to obtain the third-order current density $\vec{J}^{(3)}$.

D. Magnetic-dipole moment $\vec{M}$ and the power absorbed $\mathcal{P}_{mag}$

The induced ac magnetic dipole moment $\vec{M}$, correct through second order of $\tilde{V}$, is obtained from the sum of the coefficients of $(1/r^3)\vec{Y}_{1,2}^m$ in (32) and (40) using Eqs. (58) and (42) of Ref. 7. We find

$$\vec{M} = \frac{ia^3\tilde{V}}{30}\sum_{m=-1}^{+1}\frac{\hat{e}_m^* \cdot \vec{B}_1\hat{e}_m}{1 + \frac{1}{2}m^2\tilde{\gamma} - \frac{1}{2}im\tilde{W}} - \frac{a^3\tilde{V}^2}{315}\sum_{m=-1}^{+1}\frac{\hat{e}_m^* \cdot \vec{B}_1\hat{e}_m}{(1 + \frac{1}{2}m^2\tilde{\gamma} - \frac{1}{2}im\tilde{W})^2}. \tag{41}$$

To the same order in $\tilde{V}$, we can rewrite this result in the form

$$\vec{M} = ia^3\frac{\tilde{V}}{30}\sum_{m=-1}^{+1}\frac{\hat{e}_m^* \cdot \vec{B}_1\hat{e}_m}{1 + \frac{1}{2}m^2\tilde{\gamma} - \frac{1}{2}im\tilde{W} - i\frac{2}{21}\tilde{V}}. \tag{42}$$

We find that this second form for $\vec{M}$ is accurate to much larger $\tilde{V}$ than (41) by comparison with the exact solutions.[4] Numerical examples of the region of validity of (42) are given in Sec. VI.

The mean power absorbed by the sphere is

$$\mathcal{P}_{mag} = \tfrac{1}{2}\omega\,\mathrm{Im}\vec{M} \cdot \vec{B}_1^*. \tag{43}$$

Using (42), this becomes

$$\mathcal{P}_{mag} = \frac{\omega a^3}{30}\sum_{m=-1}^{1}|\hat{e}_m^* \cdot \vec{B}_1|^2 \times \mathrm{Re}\left(\frac{\tilde{V}}{2 + m^2\tilde{\gamma} - im\tilde{W} - i\frac{4}{21}\tilde{V}}\right). \tag{44}$$

Here Re and Im stand for real and imaginary parts, respectively. Each term in the sum in this formula corresponds to the power absorbed by a definite circular polarization of the exciting ac field $\vec{B}_1$. For a linearly polarized exciting field ($\vec{B}_1$ real) this formula can be written

$$\mathcal{P}_{\text{mag}}=\frac{\omega a^3}{30}\left[(\hat{z}\cdot\vec{B}_1)^2\,\mathrm{Re}\left(\frac{\tilde{V}}{2-i\frac{4}{21}\tilde{V}}\right)\right.$$
$$\left.+[B_1^2-(\hat{z}\cdot\vec{B}_1)^2]\,\mathrm{Re}\left(\frac{\tilde{V}(2+\tilde{\gamma}-i\frac{4}{21}\tilde{V})}{(2+\tilde{\gamma}-i\frac{4}{21}\tilde{V})^2+\tilde{W}^2}\right)\right]. \tag{45}$$

This is the formula we use in discussing the experimental results in Sec. VI.

IV. ELECTRIC EXCITATION

Here we consider the electric-excitation problem, which is the complement of the magnetic-excitation problem treated in Sec. III. The gyrotropic sphere is now excited by a uniform ac electric field $\vec{E}_1 e^{-i\omega t}$, and we wish to determine the leading terms in the *electric* multipole response.

A. Perturbation scheme

When the frequency is very low- (or the sphere radius is small), we can neglect the magnetic-induction field in (10) or, equivalently, in (11). The zeroth-order total current density inside the sphere therefore satisfies the equation:

$$\mathrm{curl}(\vec{J}^{(0)}+\tilde{\gamma}\hat{z}\cdot\vec{J}^{(0)}\hat{z}+\tilde{W}\hat{z}\times\vec{J}^{(0)})=0\,. \tag{46}$$

Outside the sphere,

$$\vec{J}^{(0)}=-i(\omega/4\pi)\vec{E}^{(0)}\,, \tag{47}$$

where $\vec{E}^{(0)}$ satisfies the quasistatic equations (15). The boundary conditions (17a) and (17b) then determine $\vec{J}^{(0)}$ everywhere.

The first-order total current density inside the sphere satisfies the helicon wave equation (12) in which the source term on the right-hand side is given by the zeroth-order solution:

$$\mathrm{curl\,curl}(\vec{J}^{(1)}+\tilde{\gamma}\hat{z}\times\vec{J}^{(1)}\hat{z}+\tilde{W}\hat{z}\times\vec{J}^{(1)})=\tilde{q}_0^2\vec{J}^{(0)}\,. \tag{48}$$

Outside the sphere,

$$\vec{J}^{(1)}=-i(\omega/4\pi)\vec{E}^{(1)}\,, \tag{49}$$

where $\vec{E}^{(1)}$ satisfies the quasistatic equations (15). The boundary conditions (17a) and (17b) then fix the solution everywhere.

The higher-order equations are obtained by advancing the index in (48) and (49).

B. Zeroth-order solution

Outside the sphere, the zeroth-order electric field is the sum of the applied uniform electric field $\vec{E}_1$ and the field of an electric dipole:

$$\vec{E}^{(0)}=(4\pi)^{1/2}\sum_{m=-1}^{1}\hat{e}_m^*\cdot\vec{E}_1\vec{Y}_{1,0}^m$$
$$+\sum_{m=-1}^{1}f_1^m\left(\frac{a}{r}\right)^3\vec{Y}_{1,2}^m\,, \tag{50}$$

where the coefficients f_1^m are yet to be determined. Inside the sphere the zeroth order total current density must be the constant vector:

$$\vec{J}^{(0)}=\sum_{m=-1}^{1}g_1^m\vec{Y}_{1,0}^m\,, \tag{51}$$

where the coefficients g_1^m are yet to be determined. To establish this form note first that the operations $\hat{r}\cdot$ and $\hat{r}\times$ appearing in the boundary conditions (17a) and (17b) do not change the index L of $\vec{Y}_{L,l}^m$ [see Eqs. (A10) and (A11)]. Also, the parity, which is the parity of the index l, must be the same inside and outside the sphere. Thus $L=1$ and $l=0$ or 2. But, from the formulas (B11) of Ref. 7, we see that the divergence of $\vec{Y}_{1,2}^m$ is not zero, so (51) is the most general form.

Using the generalized Ohm-Hall law (7) and noting the formulas for $\hat{z}\times\vec{Y}_{L,l}^m$ in Appendix B of Ref. 7 and for $\hat{z}\cdot\vec{Y}_{L,l}^m\hat{z}$ in Appendix A, we get for the zeroth-order electric field inside the sphere

$$\vec{E}^{(0)}=\sum_{m=-1}^{1}g_1^m\frac{1+\tilde{\gamma}(1-m^2)-im\tilde{W}}{\tilde{\sigma}}\vec{Y}_{1,0}^m\,. \tag{52}$$

Applying the boundary conditions (17a) and (17b) and using the formulas (A10) and (A11), we get two equations for the coefficients f_1^m and g_1^m; the solution is

$$f_1^m=(8\pi)^{1/2}\frac{1+(1-m^2)\tilde{\gamma}-im\tilde{W}-\tilde{\epsilon}}{2[1+(1-m^2)\tilde{\gamma}-im\tilde{W}]+\tilde{\epsilon}}\;\hat{e}_m^*\cdot\vec{E}_1\,, \tag{53}$$

$$g_1^m=(4\pi)^{1/2}\frac{3\tilde{\sigma}}{2[1+(1-m^2)\tilde{\gamma}-im\tilde{W}]+\tilde{\epsilon}}\;\hat{e}_m^*\cdot\vec{E}_1\,, \tag{54}$$

where

$$\tilde{\epsilon}\equiv i(4\pi\tilde{\sigma}/\omega). \tag{55}$$

C. First-order solution

We determine $\vec{J}^{(1)}$ inside the sphere from (48) in which $\vec{J}^{(0)}$ is given by (51). The general form of this solution is

$$\vec{J}^{(1)}=\sum_{m=-1}^{1}[d_0^m a^2\vec{Y}_{1,0}^m+d_1^m r^2(\vec{Y}_{1,2}^m+\tfrac{5}{\sqrt{2}}\vec{Y}_{1,0}^m)$$
$$+d_2^m r^2\vec{Y}_{2,2}^m+d_3^m r^2\vec{Y}_{3,2}^m]\,, \tag{56}$$

where $d_0^m\ldots d_3^m$ are yet to be determined. To establish this form, note, from the formulas (B12) of Ref. 7 for the curl, that the operation curl curl shifts the index l of $\vec{Y}_{L,l}^m$ by 0 or 2 while the operations $\hat{z}\cdot\vec{Y}_{L,l}^m\hat{z}$ and $\hat{z}\times\vec{Y}_{L,l}^m$ leave the index l unchanged. Hence, $\vec{J}^{(1)}$ can involve only $\vec{Y}_{L,l}^m$ with $l=0$ or 2. The form (56) then follows from the requirements that $\vec{J}^{(1)}$ be regular at the origin and have vanished divergence.

Substituting the form (56) into (48) gives the relation

$$a_{11}d_1^m + a_{12}d_2^m + a_{13}d_3^m = -\tilde{q}_0^2 g_1^m/(5\sqrt{2}), \tag{57}$$

where

$$a_{11} = 3 + 2[1 - m^2 + \tfrac{1}{20}(4 - m^2)]\tilde{\gamma} - \tfrac{3}{2}im\tilde{W},$$
$$a_{12} = -\tfrac{1}{2}[(4 - m^2)/15]^{1/2}(m\tilde{\gamma} - 3i\tilde{W}),$$
$$a_{13} = -[(4 - m^2)(9 - m^2)/150]^{1/2}\tilde{\gamma}. \tag{58}$$

Outside the sphere the first-order electric field is the sum of a dipole and an octupole field:

$$\vec{E}^{(1)} = \sum_{m=-1}^{1} h_1^m \left(\frac{a}{r}\right)^3 \vec{Y}_{1,2}^m + \sum_{m=-1}^{1} h_3^m \left(\frac{a}{r}\right)^5 \vec{Y}_{3,4}^m. \tag{59}$$

From the boundary condition (17a), using (49), we get two relations

$$\sqrt{2}\,d_0^m + 3d_1^m = (i\omega/2\pi a^2)h_1^m, \tag{60}$$
$$\sqrt{3}\,d_3^m = (i\omega/2\pi a^2)h_3^m. \tag{61}$$

From the boundary condition (17b), using the generalized Ohm-Hall law (7), we get three more relations which can be written

$$a_{11}d_1^m + a_{12}d_2^m + a_{13}d_3^m = (\tilde{\sigma}/a^2)h_1^m - [1 + (1 - m^2)\tilde{\gamma} - im\tilde{W}] \times (\sqrt{2}\,d_0^m + 3d_1^m), \tag{62}$$

$$a_{12}d_1^m + a_{22}d_2^m + a_{23}d_3^m = 0, \tag{63}$$

$$a_{13}d_1^m + a_{23}d_2^m + a_{33}d_3^m = \tfrac{1}{2}\sqrt{3}(\tilde{\sigma}/a^2)h_3^m + \tfrac{3}{4}\tilde{\epsilon}\,d_3^m, \tag{64}$$

where

$$a_{22} = 1 + \tfrac{1}{8}m^2\tilde{\gamma} - i\tfrac{1}{8}m\tilde{W},$$
$$a_{23} = \tfrac{1}{3}[(9 - m^2)/10]^{1/2}(m\tilde{\gamma} + 2i\tilde{W}),$$
$$a_{33} = 1 + \tfrac{3}{4}\tilde{\epsilon} + \tfrac{1}{15}(9 - m^2)\tilde{\gamma} - i\tfrac{1}{3}m\tilde{W}. \tag{65}$$

The six equations (57) and (60)–(64) serve to determine the six coefficients d_0^m, d_1^m, d_2^m, d_3^m, h_1^m, and h_3^m. Here, however, we need only obtain an explicit expression for h_1^m, the dipole-moment coefficient. To do this we note that since the left-hand sides of (57) and (62) are identical, their right-hand sides must be equal. But, using (60), the right-hand side of (62) can be expressed in terms of h_1^m alone. Solving the resulting equation we find

$$h_1^m = -i\frac{4\pi\tilde{q}_0^2 a^2}{5\sqrt{2}\omega}\,\frac{g_1^m}{2[1 + (1 - m^2)\tilde{\gamma} - im\tilde{W}] + \tilde{\epsilon}}, \tag{66}$$

where we have used (55). Comparing (13) and (20) we see that $\tilde{q}_0^2 a^2 = i\tilde{V}$. Then inserting the expression (54) for g_1^m, we can write

$$h_1^m = -i\frac{3\sqrt{2\pi}}{5}\tilde{V}\,\frac{\tilde{\epsilon}\hat{e}_m^* \cdot \vec{E}_1}{\{2[1 + (1 - m^2)\tilde{\gamma} - im\tilde{W}] + \tilde{\epsilon}\}^2}, \tag{67}$$

where again we have used (55).

D. Electric-dipole moment $\vec{P}$ and the power absorbed $\mathcal{P}_{\text{elect}}$

The electric-dipole moment $\vec{P}$ is related to the coefficients f_1^m and h_1^m exactly as the magnetic-dipole moment $\vec{M}$ is related to the corresponding coefficients in the magnetic field [see Eq. (58) of Ref. 7],

$$\vec{P} = -\frac{a^3}{(8\pi)^{1/2}}\sum_{m=-1}^{1}(f_1^m + h_1^m)\hat{e}_m. \tag{68}$$

Using (53) and (67), we have

$$\vec{P} = -a^3\sum_{m=-1}^{1}\hat{e}_m^* \cdot \vec{E}_1\,\hat{e}_m\left(\frac{1 + (1 - m^2)\tilde{\gamma} - im\tilde{W} - \tilde{\epsilon}}{2[1 + (1 - m^2)\tilde{\gamma} - im\tilde{W}] + \tilde{\epsilon}} - i\tfrac{3}{10}\tilde{V}\frac{\tilde{\epsilon}}{\{2[1 + (1 - m^2)\tilde{\gamma} - im\tilde{W}] + \tilde{\epsilon}\}^2}\right). \tag{69}$$

As in the magnetic case, we can, to the same order in $\tilde{V}$, write this in the more compact form

$$\vec{P} = -a^3\sum_{m=-1}^{1}\hat{e}_m^* \cdot \vec{E}_1\,\hat{e}_m\,\frac{1 + (1 - m^2)\tilde{\gamma} - im\tilde{W} - \frac{1}{10}i\tilde{V} - \tilde{\epsilon}}{2[1 + (1 - m^2)\tilde{\gamma} - im\tilde{W} - \frac{1}{10}i\tilde{V}] + \tilde{\epsilon}}. \tag{70}$$

As in the magnetic case, this expression is numerically more accurate than the less compact form (69).

The mean power absorbed by the sphere is

$$\mathcal{P}_{\text{elect}} = \tfrac{1}{2}\omega\,\text{Im}\,\vec{P} \cdot \vec{E}_1^*. \tag{71}$$

Using (70), we can write

$$\mathcal{P}_{\text{elect}} = \tfrac{3}{4}\omega a^3\sum_{m=-1}^{1}|\hat{e}_m^* \cdot \vec{E}_1|^2\,\text{Im}\,\frac{\tilde{\epsilon}}{2[1 + (1 - m^2)\tilde{\gamma} - im\tilde{W} - \frac{1}{10}i\tilde{V}] + \tilde{\epsilon}}. \tag{72}$$

Specializing to the case of a linearly polarized electric field ($\vec{E}_1$ real), we can write

$$\mathcal{P}_{\text{elect}} = \tfrac{3}{4}\omega a^3\left((\hat{z} \cdot \vec{E}_1)^2\,\text{Im}\,\frac{\tilde{\epsilon}}{2(1 + \tilde{\gamma} - \frac{1}{10}i\tilde{V}) + \tilde{\epsilon}} + [E_1^2 - (\hat{z} \cdot \vec{E}_1)^2]\,\text{Im}\,\frac{\tilde{\epsilon}(2 - \frac{1}{5}i\tilde{V} + \tilde{\epsilon})}{(2 - \frac{1}{5}i\tilde{V} + \tilde{\epsilon})^2 + 4\tilde{W}^2}\right). \tag{73}$$

This formula together with (45) are the basic results we use in the discussion of experimental results in Sec. VI.

V. SPECIALIZATION TO DEGENERATE ELECTRON GAS

Although the formulas (45) for $\mathcal{P}_{mag}$ and (73) for $\mathcal{P}_{elect}$ have a fairly simple mathematical structure, the detailed dependence on ω, a, and B_0, and on the electrical parameters μ, ϵ_l, N, and m^* is very intricate. As a first step in trying to understand how the power absorbed depends on these seven parameters, in this section we consider the case where the electron gas is highly degenerate. The electron relaxation time is then a single number, and the average over energy in (4a)–(4c) is not necessary.

A. Parameters $\tilde{V}$, $\tilde{\gamma}$, $\tilde{W}$, $\tilde{\epsilon}$

The dc electrical conductivity is

$$\sigma_0 = (N e^2 \tau_0 / m^*) = N e \mu, \tag{74}$$

where τ_0 is the electron relaxation time and μ is the mobility at $\omega = 0$. If we define the following dimensionless parameters:

$$\begin{aligned} &U_0 \equiv \omega \tau_0, \quad V_0 \equiv 4\pi\omega\sigma_0 (a/c)^2, \\ &W_0 \equiv \omega_c \tau_0, \quad X_0 \equiv \omega \epsilon_l / 4\pi\sigma_0, \end{aligned} \tag{75}$$

the coefficients C_j defined in Sec. II become

$$\begin{aligned} C_1 &= \sigma_0 \left(\frac{(1 - i U_0)^2}{(1 - i U_0)^2 + W_0^2} - i X_0 \right), \\ C_2 &= \frac{\sigma_0 W_0^2}{(1 - i U_0)[(1 - i U_0)^2 + W_0^2]}, \\ C_3 &= \frac{\sigma_0 W_0}{(1 - i U_0)^2 + W_0^2}. \end{aligned} \tag{76}$$

Using these results, the definitions (8) of $\tilde{\sigma}$, $\tilde{\gamma}$, and $\tilde{W}$, and the definition of $\tilde{V}$ and $\tilde{\epsilon}$ given by (20) and (55) respectively, we find

$$\begin{aligned} \tilde{V} &= V_0 \frac{[1 - i X_0 (1 - i U_0)]^2 - X_0^2 W_0^2}{(1 - i U_0)[1 - i X_0 (1 - i U_0)] - i X_0 W_0^2}, \\ \tilde{\gamma} &= \frac{i X_0 W_0^2}{[1 - i X_0 (1 - i U_0)]\{(1 - i U_0)[1 - i X_0 (1 - i U_0)] - i X_0 W_0^2\}}, \\ \tilde{W} &= \frac{W_0}{(1 - i U_0)[1 - i X_0 (1 - i U_0)] - i X_0 W_0^2}, \\ \tilde{\epsilon} &= \epsilon_l \frac{X_0^2 W_0^2 - [1 - i X_0 (1 - i U_0)]^2}{X_0^2 W_0^2 + (1 - i U_0)[X_0^2 (1 - i U_0) + i X_0]}. \end{aligned} \tag{77}$$

B. Magnetic excitation

It is clear that to write out the formula for $\mathcal{P}_{mag}$, explicitly exhibiting the dependence of U_0, V_0, W_0, and X_0, is still a considerable algebraic task. To simplify things a bit, we note that in a typical narrow-gap semiconductor such as InSb, X_0 is generally a fairly small number (~ 0.05 for the experiments of interest to us here). Thus, if we neglect X_0 in the expressions for $\tilde{V}$, $\tilde{\gamma}$, and $\tilde{W}$ (which corresponds to neglecting displacement current), then one can show that in the transverse magnetic geometry ($\vec{B}_0 \perp \vec{B}_1$)

$$\mathcal{P}_{mag}(\text{trans.}) = \frac{\omega B_1^2 a^3 V_0}{120} \left(\frac{1}{(U_0 + \frac{2}{21} V_0 + \frac{1}{2} W_0)^2 + 1} + \frac{1}{(U_0 + \frac{2}{21} V_0 - \frac{1}{2} W_0)^2 + 1} \right). \tag{78}$$

It is clear that the second term peaks when

$$W_0 = 2U_0 + \tfrac{4}{21} V_0. \tag{79}$$

Using the definitions (74) and (75) we can write this resonance condition as

$$\omega_c = 2\omega + \tfrac{4}{21} \omega \omega_p^2 (a^2/c^2). \tag{80}$$

Here ω_p [$= (4\pi N e^2/m^*)^{1/2}$] is the plasma frequency. Thus, the resonance field varies quadratically with the sphere radius, and at very small a it approaches[8]

$$B_0(\text{resonance}) = 2\omega m^* c/e. \tag{81}$$

Consequently, this transverse magnetic resonance can be used to determine the effective mass m^*. The potential usefulness of this idea was first realized by Evans, Furdyna, and Galeener.[1] In the real experimental situation, the displacement current and the energy average over $\tau(\mathcal{E})$ affect these results significantly. However, these ef-

fects can readily be handled numerically.

It should be emphasized that conventional cyclotron resonance with microwaves, used for determining m^* in semiconductors, is useful only in materials with very low carrier concentration. In media such as InSb, with $N > 10^{13}$ cm^{-3}, conventional cyclotron resonance fails because of the so-called plasma shift.[3] This magnetic-dipole resonance in effect circumvents this problem, making the m^* parameter accessible to microwave experiments.

In the longitudinal magnetic case ($\vec{B}_1 \parallel \vec{B}_0$), if we were to neglect the effects of the displacement current (set $X_0 = 0$), the absorbed power would be independent of magnetic field. However, if we include X_0, it can be shown that there is a broad absorption shoulder near zero magnetic field.

C. Electric excitation

Using the expressions (77) for $\tilde{V}$, $\tilde{\gamma}$, $\tilde{W}$, and $\tilde{\epsilon}$ the formula (73) for $\mathcal{P}_{\text{elect}}$ can be written, after a great deal of algebra, in the form

$$\mathcal{P}_{\text{elect}} = \frac{6\pi a^3 \sigma_0}{(2+\alpha\epsilon_I)^2}\left((\hat{z}\cdot\vec{E}_1)^2\frac{1}{1+U'^2}+[E_1^2-(\hat{z}\cdot\vec{E}_1)^2]\frac{1+W_0^2+U'^2}{(1+W_0^2-U'^2)^2+4U'^2}\right), \tag{82}$$

where we have used the expression for X_0 in (75) and introduced

$$\alpha \equiv 1 - \tfrac{1}{5}(\omega a/c)^2, \tag{83}$$

and

$$U' \equiv \omega\tau_0 - [\alpha/(2+\alpha\epsilon_I)](\omega_p^2\tau/\omega). \tag{84}$$

The entire contribution to $\mathcal{P}_{\text{elect}}$ from the first order term in $\tilde{V}$ is contained in the size-dependent quantity α. But the basic restriction (1) of our calculation is that the wavelength outside the sphere is long compared with the sphere radius. This means that the size-dependent correction must be small, so α is close to unity. When $\alpha = 1$, the transverse part of (82) is equivalent to the well-known result of Dresselhaus, Kip, and Kittel

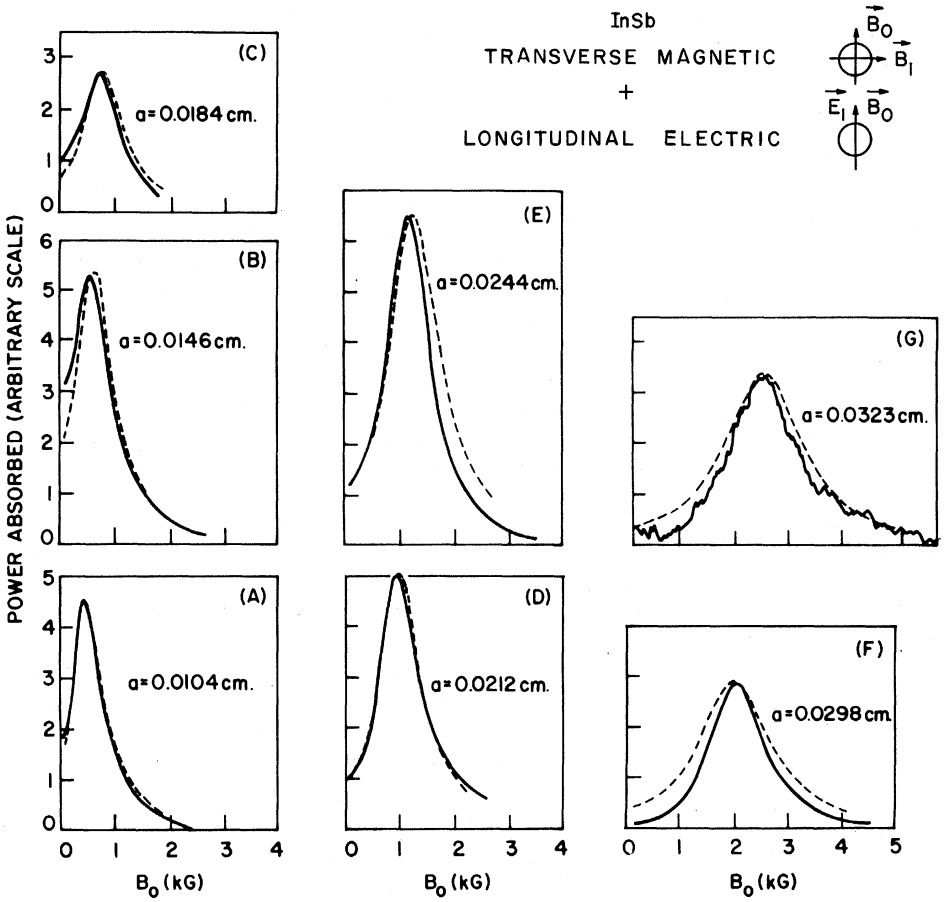

FIG. 2. Microwave absorption in one sample of n-type InSb as measured after re-etching to various smaller radii. The data (solid curves) were taken in the transverse-magnetic plus longitudinal-electric geometry ($\vec{B}_1 \perp \vec{B}_0$, $\vec{E}_1 \parallel \vec{B}_0$). The dashed curves are the theoretical fits to the data. The perturbation theory was used for A, B, C, D, while the general theory was used for the results corresponding to larger radii in E, F, G of this figure. The parameters used in this fit are $\mu = 8 \times 10^5$ cm^2/V sec, $\epsilon_I = 18$, $N = 1.7 \times 10^{14}$/cm^3, $m^* = 0.014 m_0$.

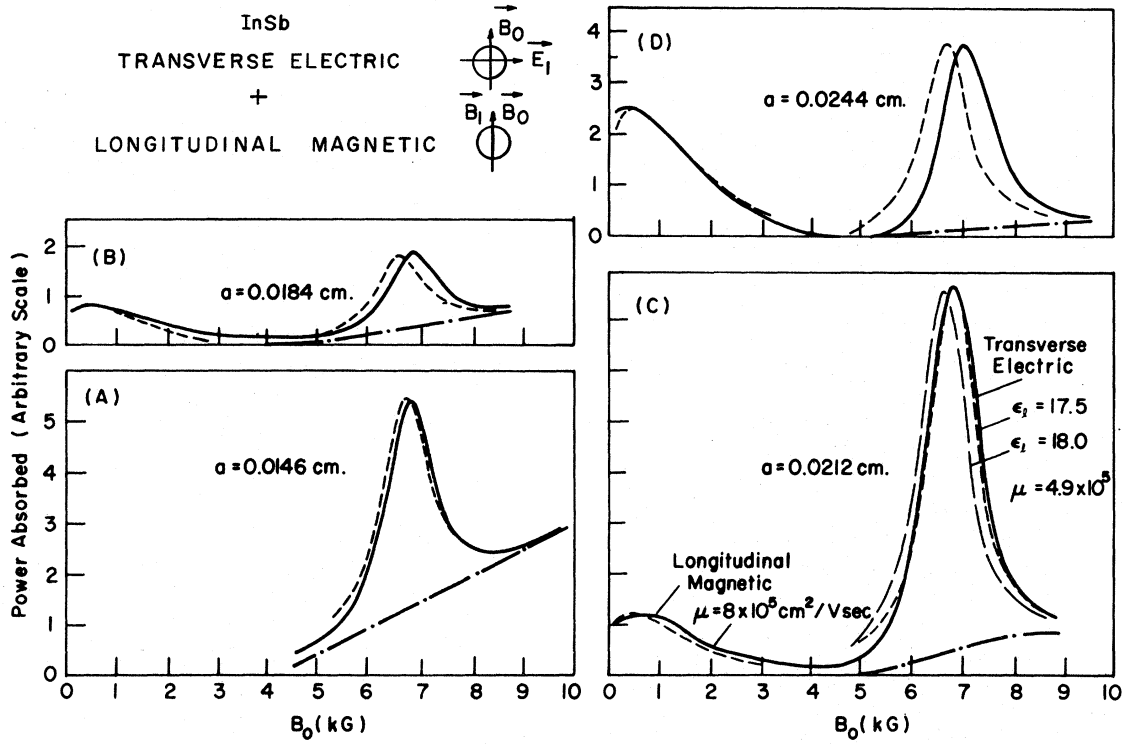

FIG. 3. Microwave absorption for the same samples as Fig. 2; however, the field geometry is transverse-electric plus longitudinal-magnetic ($\vec{E}_1 \perp \vec{B}_0$, $\vec{B}_1 \parallel \vec{B}_0$). The solid curves are the experimental traces and the dashed curves are the theory. The electrical parameters used for the theoretical fits are the same as for Fig. 2, except a lower value of $\mu = 4.9 \times 10^5$ cm^2/V sec was necessary to account for the width of the transverse-electric resonance near 7 kG. The low-field shoulder, due to longitudinal-magnetic absorption, is accounted for by using the same $\mu = 8 \times 10^5$ cm^2/V sec as in Fig. 2. The effect of a small change in ϵ_l is illustrated in C.

[their Eq. (13)].[3]

Clearly, when the quantity U' is large, the transverse part of (82) peaks when

$$W_0 \approx \pm |U'|, \tag{85}$$

or, equivalently, when

$$\omega_c \approx \pm |\omega - \alpha\omega_p^2/(2+\alpha\epsilon_l)\omega|. \tag{86}$$

In a microwave experiment involving a typical narrow band-gap semiconductor, the second term, the magnetoplasma shift, is large compared to ω, so the effect of increasing the sphere radius a, which reduces the quantity α, is to shift this electric resonance to lower magnetic fields.[9]

VI. COMPARISON WITH EXPERIMENT

In this section we compare our theoretical predictions with the original data reported in Refs. 1 and 2. In those experiments the magnetic-field dependence of the microwave absorption in small n-type InSb spheres was investigated at 78 K using a 35-GHz superheterodyne spectrometer. A rectangular microwave cavity was used in the spectrometer bridge, with linearly polarized microwave fields $\vec{B}_1$ and $\vec{E}_1$; the samples were located slightly off the position of maximum $\vec{B}_1$ in the cavity. This position allowed the observation of the response of the sphere to a transverse ac magnetic field, which was the main object of the experiments. At this same position, there was a small but finite ac electric field $\vec{E}_1$, which allowed the measurement of the much stronger transverse-electric response. Absorption or dispersion by the sample could be selectively studied by adjusting the spectrometer phase. In the case of the data discussed below, the geometry was chosen to be one of the two configurations $\vec{B}_1 \perp \vec{B}_0$, $\vec{E}_1 \parallel \vec{B}_0$ (transverse magnetic plus longitudinal electric) or $\vec{E}_1 \perp \vec{B}_0$, $\vec{B}_1 \parallel \vec{B}_0$ (transverse electric plus longitudinal magnetic).

The spherical specimens were prepared from n-type InSb single crystals of various electron concentrations by grinding in an abrasive air cylinder, and then etching down to the size desired. The dependence of the measurements upon sample size was obtained by successively re-etching to smaller radii.

In Figs. 2 and 3 we present data for a single sample at various radii. These data are representative of those obtained on more than 40 samples of various electron concentrations between 5×10^{13} and 4

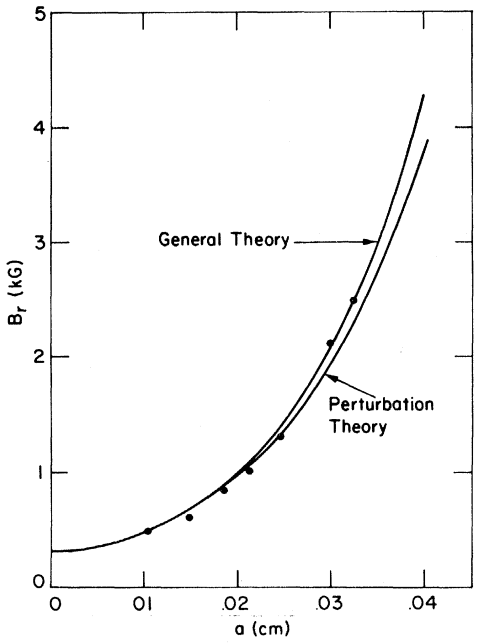

FIG. 4. Transverse-magnetic resonance field B_r corresponding to the data shown in Fig. 2 is shown here as a function of sphere radius a. The solid lines are the results of numerical calculations using the perturbation theory developed in this paper [Eq. (45)], and also of the general theory to be described in a forthcoming publication. The electrical parameters used in the calculation are those given in the caption to Fig. 2.

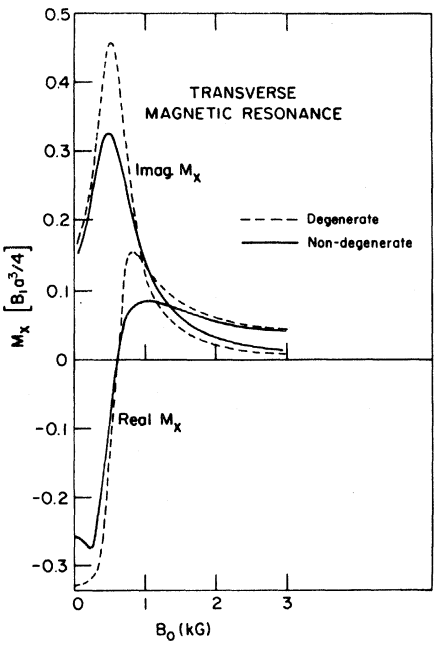

FIG. 5. This figure shows the transverse-magnetic resonance as calculated using Eq. (45) when the statistics are fully degenerate, and fully nondegenerate. Both the absorptive and the dispersive parts are shown. The parameters used in the calculation are: $\mu = 8\times10^5$ cm^2/V sec, $\epsilon_I = 18$, $N = 1.7\times10^{14}$/cm^3, $m^* = 0.014m_0$, $a = 0.0104$ cm.

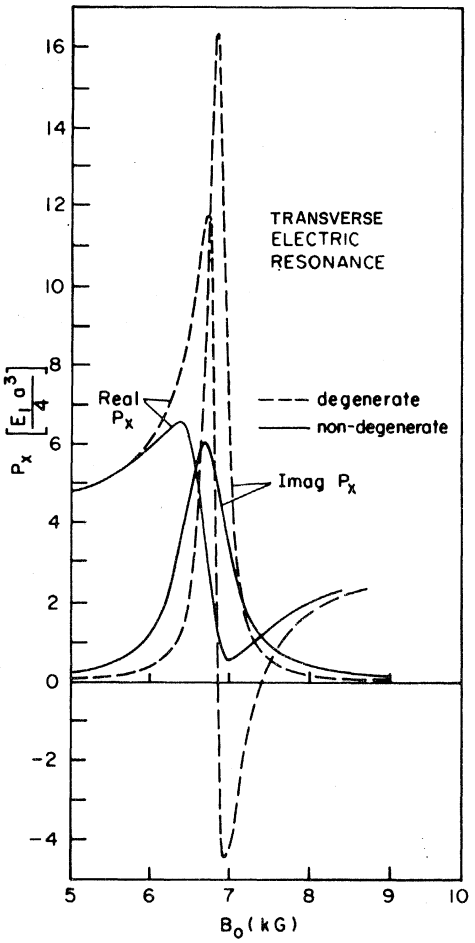

FIG. 6. This figure shows the transverse-electric resonance as calculated using Eq. (73) when the statistics are fully degenerate, and fully nondegenerate. The parameters used are the same as for Fig. 5.

$\times10^{14}$ cm^{-3}. The solid lines are replicas of the actual recorder traces of absorbed power vs applied dc magnetic field. The relative scales on the ordinate of the various traces in each figure are unrelated, since, due to the wide range of signal amplitudes, different wave-guide-cavity configurations were used in each case. However, these scales are the same for traces corresponding to the same radius in the two figures. The dash-dot lines in Fig. 3 are estimates of the sample-out background absorption. This background was negligibly small below about 5 kG, so it does not appear in Fig. 2. The dashed lines in Figs. 2 and 3 are our theoretical fit to the data.

The data shown in Fig. 2 were taken in the transverse-magnetic plus longitudinal-electric configuration. But the longitudinal-electric absorption is small and independent of field. Thus, these data can be regarded as due to transverse-magnetic absorption alone.

The theoretical curves of Fig. 3 include both transverse-electric and longitudinal-magnetic absorption. The longitudinal-magnetic absorption is negligible at fields greater than about 5 kG, but gives the low-field broad absorption shoulder. On the other hand, the transverse-electric absorption is negligible below about 5 kG, but gives the expected magnetoplasma-shifted cyclotron resonance at about 7 kG.

In the magnetic-excitation case, for spheres having radii greater than about 0.02 cm (corresponding to $|\tilde{V}| \approx 7$), there are small differences between the results of the perturbation theory given in this paper and the general theory.[4] These are illustrated by Fig. 4 in which the transverse-magnetic resonance field is plotted vs sphere radius a.

It is clear immediately that the following four general features of these experiments are explained by the theory: (a) the position and shape of the expected magnetoplasma-shifted cyclotron resonance; (b) the fact that the longitudinal-electric absorption is negligible; (c) the position, line-shape, and size dependence of the transverse-magnetic resonance; and (d) the broad absorption shoulder observed in the longitudinal-magnetic configuration.

We have found that the line shapes of both the transverse-magnetic and -electric resonances depend critically on the type of statistics which the electron gas obeys. For these experiments, the electron density is sufficiently low so that the Fermi level lies well below the bottom of the conduction band and the electron gas can be regarded as fully nondegenerate. Thus, the energy averages over the scattering time $\tau(\mathcal{E})$ required by (4) are necessary. We have assumed that the scattering is dominated by ionized-impurity Coulomb scattering and can be represented by a relaxation time proportional to $\mathcal{E}^{3/2}$.[10] With this assumption, the effect of statistics is illustrated in Figs. 5 and 6, where the absorptive and dispersive parts of the resonances are shown for the limits of fully degenerate and fully nondegenerate statistics. The parameters appropriate to the figures are given in the captions. The largest effect is in the widths and heights of the resonances; the positions are relatively insensitive to the statistics.

The data were fitted by the following procedure. The value of m^* ($=.014m_0$) was assumed to be reasonably well established.[11] The static lattice dielectric constant is somewhat controversial: Values from 16.6 to 19.7 appear in the literature,[12] with the value 17.8, recently reported by Glover and Champlin, perhaps the most reliable. We chose $\epsilon_l = 18$ as a compromise. With these parameters fixed we then adjusted the remaining parameter N and μ. All the theoretical curves of Figs. 2 and 3 were obtained with $N = 1.7 \times 10^{14}$ cm^{-3}, which agrees with the manufacturer's nominal specifications [$N = (1.5\text{–}2.5) \times 10^{14}$ cm^{-3}] for this sample at 78 K. Numerically, we found that the widths of the transverse-magnetic and -electric resonances are largely determined by the dc mobility μ and relatively insensitive to the other parameters. A value of $\mu = 8 \times 10^5$ cm^2/V sec (which is reasonable for relatively pure InSb material at 78 K) accounts for the series of transverse-magnetic resonances of Fig. 2. However, a lower value $\mu = 4.9 \times 10^5$ cm^2/V sec was necessary to account for the widths of the transverse electric peaks of Fig. 3 which occur at a considerably higher field. This would indicate that τ depends on the magnetic field, a suggestion which seems to have some other experimental support.[13,14]

The position of the electric resonance is primarily determined by N/ϵ_l, and since we have fixed ϵ_l at 18, this determined N. On the other hand, the position of the transverse-magnetic resonance is determined primarily by m^*. The scaling of the ordinate was done by fitting the theory to the experiment at the peaks of the transverse-magnetic and -electric resonances. Once this was done the scale factor for the longitudinal-magnetic absorption shoulder of Fig. 3 was fixed.

Although the above fitting procedure should be regarded as the first step of a more sophisticated search for the optimum set of parameters μ, ϵ_l, m^*, and N, proceeding beyond this point is not justified here because of uncertainties in the data. Among these are the phase setting of the microwave spectrometer, which selects the absorptive component of the signal, was determined only to within about 5°; the precise zero level and field dependence of the background were not well established; the calibration of the dc magnetic field was not sufficiently precise; and finally, there are small uncertainties in sample size and sphericity. In future experiments these experimental uncertainties could be largely eliminated.

Finally, it is appropriate to add that a number of other experimental features, not illustrated by Figs. 1–3 but reported in Refs. 1 and 2, are also confirmed by the theory. These are (a) the excitations $\vec{B}_1 \perp \vec{B}_0$, $\vec{B}_1 \parallel \vec{B}_0$, and $\vec{E}_1 \perp \vec{B}_0$ are, respectively, linearly independent; (b) the transverse-magnetic resonance is excited by the component of $\vec{B}_1$ which is circularly polarized in the cyclotron-resonance-active sense, while the plasma-shifted cyclotron resonance is (as is well known) excited by cyclotron-resonance-inactive circular component of $\vec{E}_1$; and (c) the resonance amplitude of the transverse magnetic resonance in the Rayleigh limit is proportional to the fifth power of a.

VII. CONCLUDING REMARKS

It is clear from the above comparison (Sec. VI) that the theory developed in this paper agrees with

all the observed features of microwave absorption in small gyrotropic semiconductor spheres. Essential in obtaining this agreement was the incorporation in the theory of the effects of displacement current and an energy-dependent relaxation time.

With this precision theory it is now possible that accurate values of the four electrical parameters m^*, ϵ_l, N, and μ can be obtained for a given sample from one microwave experiment. In addition, it appears that information regarding the nature of the carrier-scattering mechanisms can be obtained from detailed fits of the absorption spectrum.

ACKNOWLEDGMENT

The authors are grateful to Dr. T. A. Evans, whose original data were used in Figs. 2 and 3, for the use of these materials and for several valuable comments.

APPENDIX A: VECTOR SPHERICAL HARMONICS

For completeness and clarity, we reproduce some of the necessary elementary formulas for the vector spherical harmonics. The reader should refer to Appendix B of Ref. 7 for additional formulas. We have found the book by Edmonds particularly helpful on these functions.[15] The vector spherical harmonics are defined by

$$\vec{Y}^m_{l+1,l}=\left(\frac{(l+m)(l+m+1)}{2(l+1)(2l+1)}\right)^{1/2}Y_l^{m-1}\hat{e}_1+\left(\frac{(l-m+1)(l+m+1)}{(l+1)(2l+1)}\right)Y_l^m\hat{e}_0+\left(\frac{(l-m)(l-m+1)}{2(l+1)(2l+1)}\right)^{1/2}Y_l^{m+1}\hat{e}_{-1}, \tag{A1}$$

$$\vec{Y}^m_{l,l}=-\left(\frac{(l+m)(l-m+1)}{2l(l+1)}\right)^{1/2}Y_l^{m-1}\hat{e}_1+\frac{m}{[l(l+1)]^{1/2}}Y_l^m\hat{e}_0+\left(\frac{(l-m)(l+m+1)}{2l(l+1)}\right)^{1/2}Y_l^{m+1}\hat{e}_{-1}, \tag{A2}$$

$$\vec{Y}^m_{l-1,l}=\left(\frac{(l-m)(l-m+1)}{2l(2l+1)}\right)^{1/2}Y_l^{m-1}\hat{e}_1-\left(\frac{(l-m)(l+m)}{l(2l+1)}\right)^{1/2}Y_l^m\hat{e}_0+\left(\frac{(l+m)(l+m+1)}{2l(2l+1)}\right)^{1/2}Y_l^{m+1}\hat{e}_{-1}. \tag{A3}$$

The basis vectors $\hat{e}_m$ are given by

$$\hat{e}_1=-2^{-1/2}(\hat{x}+i\hat{y}),\quad \hat{e}_0=\hat{z},\quad \hat{e}_{-1}=2^{-1/2}(\hat{x}-i\hat{y}), \tag{A4}$$

and the usual (scalar) spherical harmonics are

$$Y_l^m(\theta,\varphi)=(-)^m[(2l+1)(l-m)!/4\pi(l+m)!]^{1/2}P_l^m(\cos\theta)\,e^{im\varphi}, \tag{A5}$$

where the associated Legendre functions are given by the Rodrigues formula

$$P_l^m(x)=[(1-x^2)^{m/2}/2^l l!](d^{l+m}/dx^{l+m})(x^2-1)^l. \tag{A6}$$

The following formulas (in addition to the formulas for $\hat{z}\times\vec{Y}^m_{l,l}$ in Appendix B of Ref. 7) are necessary in order to construct the electric field $\vec{E}$ from the current density $\vec{J}$ in Secs. III and IV:

$$\vec{Y}^m_{l+1,l}\cdot\hat{z}\hat{z}=\frac{(l-m+1)(l+m+1)}{(l+1)(2l+1)}\vec{Y}^m_{l+1,l}+m\left(\frac{(l-m+1)(l+m+1)}{l(l+1)^2(2l+1)}\right)^{1/2}\vec{Y}^m_{l,l}-\left(\frac{(l-m+1)(l+m+1)(l^2-m^2)}{l(l+1)(2l+1)^2}\right)^{1/2}\vec{Y}^m_{l-1,l}, \tag{A7}$$

$$\vec{Y}^m_{l,l}\cdot\hat{z}\hat{z}=m\left(\frac{(l-m+1)(l+m+1)}{l(l+1)^2(2l+1)}\right)^{1/2}\vec{Y}^m_{l+1,l}+\frac{m^2}{l(l+1)}\vec{Y}^m_{l,l}-m\left(\frac{l^2-m^2}{l^2(l+1)(2l+1)}\right)^{1/2}\vec{Y}^m_{l-1,l}, \tag{A8}$$

$$\vec{Y}^m_{l-1,l}\cdot\hat{z}\hat{z}=\left(\frac{(l-m+1)(l+m+1)(l^2-m^2)}{l(l+1)(2l+1)^2}\right)^{1/2}\vec{Y}^m_{l+1,l}-\left(\frac{(l-m)(l+m+1)(l^2-m^2)}{2l^2(l+1)(2l+1)}\right)^{1/2}\vec{Y}^m_{l,l}+\left(\frac{l^2-m^2}{l(2l+1)}\right)\vec{Y}^m_{l-1,l}. \tag{A9}$$

The following formulas are necessary in satisfying the boundary conditions in the electric-excitation problem:

$$\hat{r}\cdot\vec{Y}^m_{l,l-1}=[l/(2l+1)]^{1/2}Y_l^m,\quad \hat{r}\cdot\vec{Y}^m_{l,l}=0,\quad \hat{r}\cdot\vec{Y}^m_{l,l+1}=-[(l+1)/(2l+1)]^{1/2}Y_l^m, \tag{A10}$$

and

$$\begin{aligned}\hat{r}\times\vec{Y}^m_{l,l-1}&=i[(l+1)/(2l+1)]^{1/2}\vec{Y}^m_{l,l},\\ \hat{r}\times\vec{Y}^m_{l,l}&=i\{[l/(2l+1)]^{1/2}\vec{Y}^m_{l,l+1}+[(l+1)/(2l+1)]^{1/2}\vec{Y}^m_{l,l-1}\},\\ \hat{r}\times\vec{Y}^m_{l,l+1}&=i[l(2l+1)]^{1/2}\vec{Y}^m_{l,l}.\end{aligned} \tag{A11}$$

APPENDIX B: DIELECTRIC-TENSOR NOTATION

In microwave and infrared experiments it is common practice to write the inverse of the Ohm-Hall law (7) in terms of the so-called "dielectric tensor" $\vec{\epsilon}$. If we write

$$\vec{J} = -(i\omega/4\pi)\overleftrightarrow{\epsilon}\cdot\vec{E}, \tag{B1}$$

we note immediately from Eqs. (2) and (3) that

$$\epsilon_{xx} = i(4\pi/\omega)C_1, \quad \epsilon_{xy} = -i(4\pi/\omega)C_3, \quad \epsilon_{zz} = i(4\pi/\omega)(C_1 + C_2), \tag{B2}$$

and the form of $\overleftrightarrow{\epsilon}$ is

$$\overleftrightarrow{\epsilon} = \begin{pmatrix} \epsilon_{xx} & \epsilon_{xy} & 0 \\ -\epsilon_{xy} & \epsilon_{xx} & 0 \\ 0 & 0 & \epsilon_{zz} \end{pmatrix}. \tag{B3}$$

In the coordinate system described by the basis vectors $\hat{e}_1$, $\hat{e}_{-1}$, $\hat{e}_0$, the tensor $\overleftrightarrow{\epsilon}$ is diagonal:

$$\overleftrightarrow{\epsilon} = \begin{pmatrix} \epsilon_{+1} & 0 & 0 \\ 0 & \epsilon_{-1} & 0 \\ 0 & 0 & \epsilon_0 \end{pmatrix}, \tag{B4}$$

where

$$\epsilon_{\pm 1} = \epsilon_{xx} \pm i\epsilon_{xy}, \quad \epsilon_0 = \epsilon_{zz} \tag{B5}$$

In terms of the elements of $\overleftrightarrow{\epsilon}$, the parameters $\tilde{\sigma}$, $\tilde{W}$, and $\tilde{\gamma}$ are

$$\tilde{\sigma} = -\frac{i\omega}{4\pi}\frac{\epsilon_{xx}^2 + \epsilon_{xy}^2}{\epsilon_{xx}} = -\frac{i\omega}{4\pi}\frac{2\epsilon_{+1}\epsilon_{-1}}{\epsilon_{+1} + \epsilon_{-1}},$$

$$\tilde{W} = \frac{\epsilon_{xy}}{\epsilon_{xx}} = i\frac{\epsilon_{-1} - \epsilon_{+1}}{\epsilon_{-1} + \epsilon_{+1}}, \tag{B6}$$

$$\tilde{\gamma} = \frac{\epsilon_{xx}^2 + \epsilon_{xy}^2}{\epsilon_{xx}\epsilon_{zz}} - 1 = \frac{2\epsilon_{+1}\epsilon_{-1}}{(\epsilon_{+1} + \epsilon_{-1})\epsilon_0} - 1.$$

Furthermore, the expressions (42) and (70) for the magnetic-dipole moment $\vec{M}$ and the electric-dipole moment $\vec{P}$, respectively, can be written

$$\vec{M} = \frac{a^5}{30}\left(\frac{\omega}{c}\right)^2 \sum_{m=-1}^{+1} \frac{\epsilon_m^{(\mathrm{eff})}}{1 - \frac{2}{21}(\omega a/c)^2 \epsilon_m^{(\mathrm{eff})}} \hat{e}_m^* \cdot \vec{B}_1 \hat{e}_m, \tag{B7}$$

and

$$\vec{P} = -\tfrac{1}{2}a^3 \sum_{m=-1}^{+1} \left(1 - \frac{3\epsilon_m}{\epsilon_m + 2 - \frac{1}{5}(\omega a/c)^2 \epsilon_m}\right) \hat{e}_m^* \cdot \vec{E}_1 \hat{e}_m.$$

where

$$\epsilon_{m=\pm 1}^{(\mathrm{eff})} = 2\epsilon_{\pm 1}\epsilon_0/(\epsilon_{\pm 1} + \epsilon_0),$$

$$\epsilon_{m=0}^{(\mathrm{eff})} = 2\epsilon_{+1}\epsilon_{-1}/(\epsilon_{+1} + \epsilon_{-1}) = i(4\pi/\omega)\tilde{\sigma},$$

with ϵ_m defined by (B5).

*Supported in part by National Science Foundation, Materials Research Laboratory Program GH 33574A1 at Purdue University.

[1]T. A. Evans, F. L. Galeener, and J. K. Furdyna, *Proceedings of the XIth International Conference on Physics of Semiconductors* (Polish Scientific Publishers, Warsaw, 1972), p. 357; F. L. Galeener, T. A. Evans, and J. K. Furdyna, Phys. Rev. Lett. 29, 728 (1972).

[2]T. A. Evans and J. K. Furdyna, Phys. Rev. B 8, 1461 (1973); for additional details see T. A. Evans Ph. D. thesis (Purdue University, 1971) (unpublished).

[3]G. Dresselhaus, A. F. Kip, and C. Kittel, Phys. Rev. 98, 368 (1955); 100, 618 (1955). See also F. L. Galeener, Phys. Rev. Lett. 22, 1292 (1969).

[4]This calculation will appear in a forthcoming publication by two of us (G. W. Ford and S. A. Werner).

[5]H. C. van de Hulst, *Light Scattering by Small Particles*, (Wiley, New York, 1957), p. 75. ff.

[6]See, for example, A. C. Beer, "Galvanomagnetic Effects in Semiconductors," in *Solid State Physics*, Supp. 4, edited by F. Seitz and D. Turnbull (Academic, New York, 1963), Sec. 7, p. 32; or E. D. Palik and J. K. Furdyna, Rep. Prog. Phys. 33, 1199 ff (1970).

[7]G. W. Ford and S. A. Werner, Phys. Rev. B 8, 3702 (1973).

[8]This result was pointed out by J. K. Furdyna and J. Mycielski, Bull. Am. Phys. Soc. 19, 246 (1974). see also R. Markiewicz, Phys. Rev. B 10, 1766 (1974).

[9]This effect appears to have been observed by M. Cardona and B. Rosenblum, Phys. Rev. 129, 991 (1963).

[10]See, for example, p. 111 ff in A. C. Beer's book, Ref. 6.

[11]See, for example, E. S. Koteles and W. R. Datars, Phys. Rev. B 9, 568 (1974).

[12]N. Perrin, B. Perrin, and W. Mercouroff, in *VIIth International Conference on Physics of Semiconductors: Plasma Effects in Solids* (Dunod, Paris, 1965), p. 37; J. D. Wiley, P. S. Peercy, and R. N. Dexter, Phys. Rev. 181, 1173 (1969); J. K. Furdyna, Appl. Opt. 6, 675 (1967); G. H. Glover and K. S. Champlin, J. Appl. Phys. 40, 2315 (1969); and reference quoted therein.

[13]See A. C. Beer's book, Ref. 6, p. 99 ff, in particular Fig. 10 and the discussion associated with it.

[14]E. Pic and M. Ligeon, Phys. Status Solidi (a) 23, 409 (1974).

[15]A. R. Edmonds, *Angular Momentum in Quantum Mechanics* (Princeton University Press, Princeton, N. J., 1957).